Probabilistic Joint Recovery Method for CO_2 Plume Monitoring

1 Introduction

In order to curve current trends in climate change, it is crucial to reduce atmospheric CO_2 emissions [8]. Carbon Capture and Storage (CCS) is recognized as one of the only scalable net-negative CO_2 technologies. During injection, accurate prediction of fluid flow patterns in CCS is a challenging task, particularly due to uncertainties in CO_2 plume dynamics and reservoir properties. Monitoring techniques such as seismic imaging become imperative to understand the evolution of the CO_2 plume. Although previous time-lapse imaging methods such as the Joint Recovery Method (JRM) [5, 9, 1] have provided valuable information, however they do not communicate uncertainty thus are limited as tools for decision making. To address this, we propose the Probabilistic Joint Recovery Method (pJRM) that computes the posterior distribution at each monitoring survey while leveraging the shared structure among surveys through a shared generative model [2]. By computing posterior distributions for surveys, this method aims to provide valuable uncertainty information to decision makers in CCS projects, augmenting their workflow with principled risk minimization.

1.1 Previous Work

The JRM framework improves time-lapse imaging by leveraging the assumption that time-lapse seismic data shares common features between different surveys [5, 9] thus the joint inversion of these common features will produce a better result than independent inversion. This assumption is true for CO_2 monitoring due to the fact that large regions of the reservoirs remain unchanged i.e. regions where there is no CO_2 plume. However, the ill-posed nature of wave-based imaging used during time-lapse imaging (e.g. RTM, LS-RTM, FWI) introduces significant uncertainties that deterministic methods fail to account for. This work addresses this challenge by explicitly modeling these uncertainties, enabling more reliable subsurface property estimation.

2 Method

Inspired by previous work on reconstructing black holes utilizing shared features [3], we adopted a similar framework to solve N time-lapse problems jointly. Our approach takes N seismic measurements as input and produces N posterior distributions of the reconstructed plumes as output. To play the probabilistic counterpart of the common component in the JRM framework, the pJRM uses a Shared Generative Model (SGM) that extracts common features from the measurements. The innovation components (i.e., features unique to each survey) are captured by providing distinct latent distributions to the SGM for each monitoring survey.

2.1 Probabilistic Joint Recovery Model

Our goal is to recover the N posterior distribution CO_2 plume from the N noisy measurements. For simplicity, we illustrate the methodology using $N = 2$ time-lapse surveys, though the framework generalizes to $N \geq 2$. Mathematically, we aim to solve the two forward models jointly,

$$\mathbf{A}_1\mathbf{x}_1^* + \boldsymbol{\varepsilon}_1 = \mathbf{y}_1 \text{ and } \mathbf{A}_2\mathbf{x}_2^* + \boldsymbol{\varepsilon}_2 = \mathbf{y}_2.$$

Here, $\mathbf{x}_i^*$, where $i = 1, 2$, denotes the true acoustic properties of the subsurface, $\mathbf{y}_i$ denotes the noisy measurement obtained by applying the forward operator $\mathbf{A}_i$ to $\mathbf{x}_i^*$ with noise ε_i. Here we focus on a linear post-stack inversion operator that represents the combination of a convolution operator and a spatial derivative along traces: $\mathbf{A}_i \in \mathbb{R}^{m \times n}$, where m corresponds to the image size and n corresponds to the data size. Examples of the observed data are shown in Figures 1b and 1c. While this proof of concept uses a linear forward operator, future work will extend the framework to Full-Waveform Inversion, as it is designed to accommodate non-linear operators.

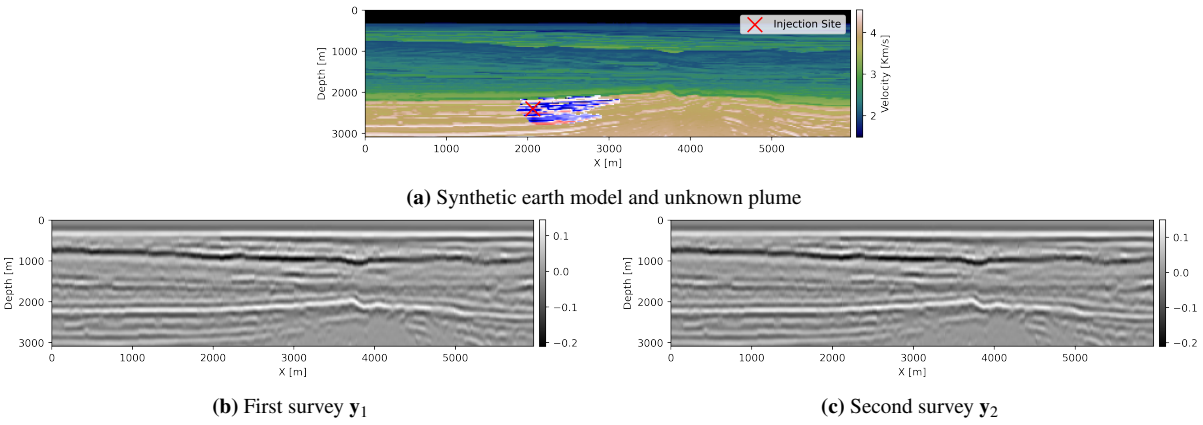

(a) Synthetic earth model and unknown plume

(b) First survey $\mathbf{y}_1$

(c) Second survey $\mathbf{y}_2$

Figure 1: Synthetic case study. (a) Earth model with CCS injection site and unknown CO_2 plume. (b) Simulated post-stack data at first survey. (c) Simulated post-stack data at second survey.

To incorporate uncertainty, we model the solutions probabilistically by using a SGM to decode latent distributions into the posterior estimates $\mathbf{x}_1$ and $\mathbf{x}_2$—i.e., $\mathbf{x}_1 \sim G_\theta(q_{\phi_1}(\mathbf{z}_1))$ and $\mathbf{x}_2 \sim G_\theta(q_{\phi_2}(\mathbf{z}_2))$, where $\mathbf{z}_i \sim \mathcal{N}(0, I)$ is the standard Gaussian distribution, and q_{ϕ_i} represents the Gaussian mixture model (GMM) used to encode the different monitors. Consequently, our objective function is defined as follows:

$$\min_{\theta,\phi_1,\phi_2} \|\mathbf{A}_1 G_\theta(q_{\phi_1}(\mathbf{z}_1)) - \mathbf{y}_1\|_2^2 + \|\mathbf{A}_2 G_\theta(q_{\phi_2}(\mathbf{z}_2)) - \mathbf{y}_2\|_2^2$$

which minimizes the difference between the forward-modeled measurements and the observed measurements with respect to the parameters θ of SGM and ϕ_i of the GMMs. After inversion for posterior distributions of $\mathbf{x}_1$ and $\mathbf{x}_2$, we take their difference to make a time-lapse image.

2.2 Probabilistic Independent Recovery Model

To evaluate the uplift in performance due to jointly solving N inverse problems versus solving them independently, we also define the Probabilistic Independent Recovery Model (pIRM):

$$\min_{\theta_1,\phi_1} \|\mathbf{A}_1 G_{\theta_1}(q_{\phi_1}(\mathbf{z}_1)) - \mathbf{y}_1\|_2^2 \text{ and } \min_{\theta_2,\phi_2} \|\mathbf{A}_2 G_{\theta_2}(q_{\phi_2}(\mathbf{z}_2)) - \mathbf{y}_2\|_2^2.$$

Here a separate generative model is trained for each time-lapse plume, while in pJRM, the generative model is shared thus extracts common features across all time-lapse surveys.

2.3 Weak formulation

When using the pJRM, the computational cost of evaluating the forward operator and its gradient at each iteration is significant. To address this, we adopted a weak formulation introduced by **(author?)**, which decouples forward operator evaluations from network parameter updates in Algorithm 1. In this approach, forward operator evaluations and gradient calculations (line 3) occur in an outer loop, while network parameter updates (line 7) take place in an inner loop. This separation reduces the total number of forward operator evaluations required, set to a relatively small value (~ 200) compared to the number of network parameter updates needed ~ 100000.

Algorithm 1 Probabilistic Joint Recovery Model (pJRM) with Weak Formulation

for $ii = 1 : \text{maxiter}_1$ **do**
  for $i = 1 : N$ **do**
    $\mathbf{g}_i = \nabla_{\mathbf{x}_i} \left[\frac{1}{2\sigma^2} \|\mathbf{A}_i(\mathbf{x}_i) - \mathbf{y}_i\|_2^2 + \frac{1}{2\gamma^2} \|\mathbf{x}_i - G_\theta \left(q_{\phi_i}(\mathbf{z}_i) \right) \|_2^2 \right]$
    $\mathbf{x}_i = \mathbf{x}_i - \tau \mathbf{g}_i$
  end for
  for $iii = 1 : \text{maxiter}_2$ **do**
    $\mathscr{L}(\phi_j, \theta) = \sum_{j=1}^{N} \left[\frac{1}{2\gamma^2} \|\mathbf{x}_j - G_\theta \left(q_{\phi_j}(\mathbf{z}_j) \right) \|_2^2 \right]$
    $(\phi_j, \theta) \leftarrow \text{ADAM}(\mathscr{L}(\phi_j, \theta))$
  end for
end for

3 Synthetic case study

We conducted in-silico validation of our method using velocity models with dimensions of $(3.2\,\text{Km} \times 5.9\,\text{Km})$, discretized into a grid of (398×103). As shown in Figure 1a, we simulated the fluid flow of CO_2 at an injection site using *Jutul*, mimicking a realistic CCS project [4]. The flow of CO_2 alters the acoustic properties of the reservoir, leading to time-lapse differences that can be imaged. To invert these time-lapse images, we employed a post-stack convolutional forward operator using *Pylops* [7]. We tested the weak formulation of our method using two and six surveys and obtained time-lapse reconstructions by taking the difference between the posterior means. To quantify uncertainty, we plotted the standard deviation of the differences between posterior samples.

Juxtaposing Figures 2b and 2c demonstrates that pJRM significantly outperforms pIRM, as previously shown in the non-probabilistic case by **(author?)** [1]. The time-lapse image generated by pJRM retains the overall shape of the CO_2 plume with lower uncertainty. In contrast, pIRM fails to capture the plume structure, resulting in high uncertainty both within the plume and across other regions of the reconstruction. Additionally, Figures 2c and 2d illustrate that increasing the number of surveys improves reconstruction quality, as the generative model benefits from observing the shared components across multiple surveys. Figure 3 further highlights a decreasing trend in uncertainties as more surveys are incorporated, validating the expected correlation between uncertainty and error. These results underscore pJRM's effectiveness in representing uncertainty, making it a more reliable tool for monitoring CCS.

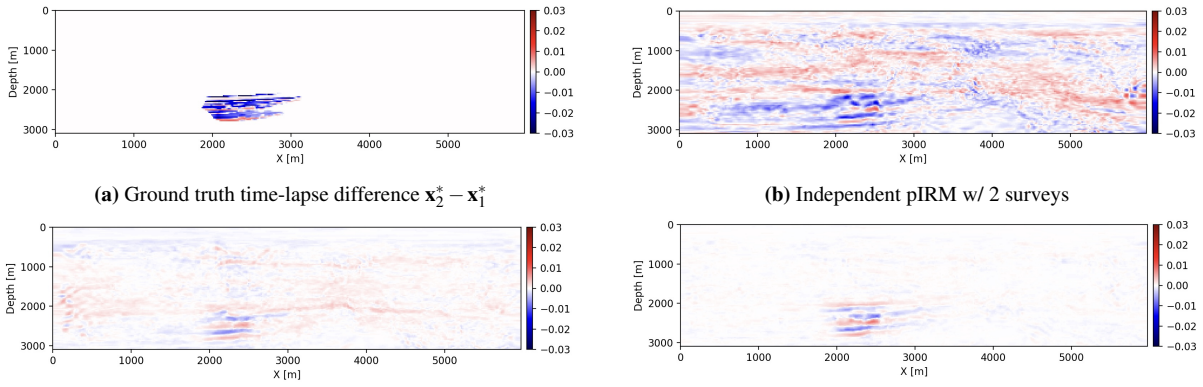

(a) Ground truth time-lapse difference $\mathbf{x}_2^* - \mathbf{x}_1^*$

(b) Independent pIRM w/ 2 surveys

(c) Joint pJRM w/ 2 surveys

(d) Joint pJRM w/ 6 surveys

Figure 2: Comparison of time-lapse Images. (a) Time-lapse image with Independent pIRM. (b) Ground truth time-lapse difference. (c) Time-lapse image with pJRM and 2 surveys. (d) Time-lapse image with pJRM and 6 surveys.

4 Conclusions

We introduce a novel approach to CCS monitoring that leverages shared structures between surveys to improve reconstruction while providing uncertainty quantification. Additionally, we present a weak formulation of the framework, enabling efficient use of computationally expensive forward operators. Our synthetic experiments

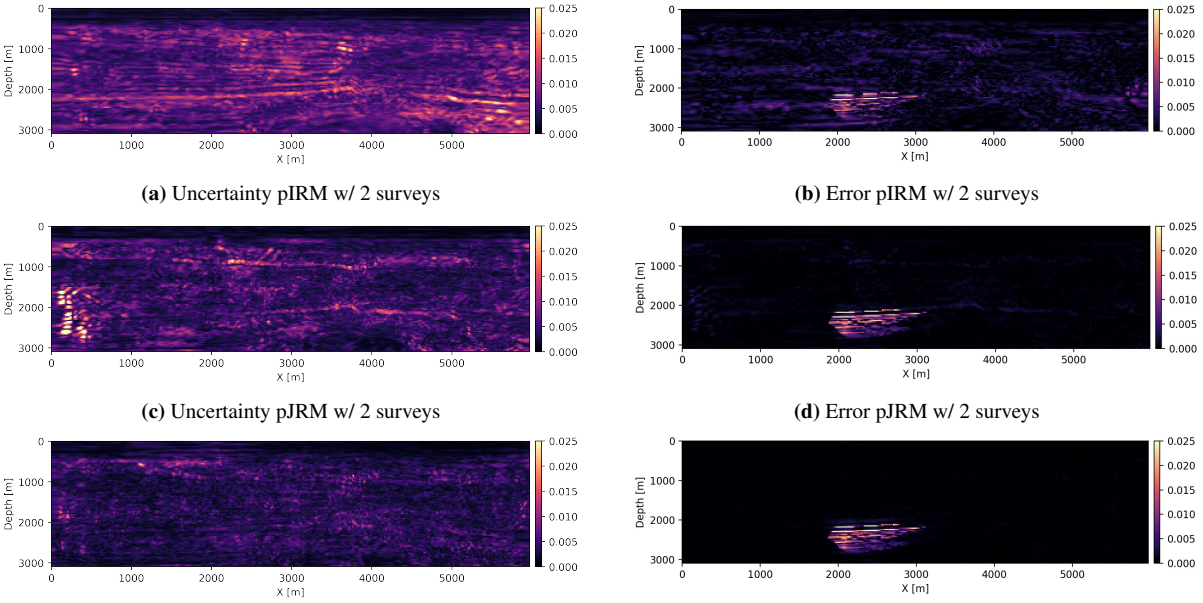

(a) Uncertainty pIRM w/ 2 surveys

(b) Error pIRM w/ 2 surveys

(c) Uncertainty pJRM w/ 2 surveys

(d) Error pJRM w/ 2 surveys

(e) Uncertainty pJRM w/ 6 surveys

(f) Error pJRM w/ 6 surveys

Figure 3: Comparison of uncertainty and errors. (a) Uncertainty of time-lapse image w/ independent method pIRM and 2 surveys. (b) Error of time-lapse image w/ pIRM and 2 surveys. (c) Uncertainty of time-lapse image w/ joint method pJRM and 2 surveys. (d) Error of time-lapse image w/ pJRM and 2 surveys. (e) Uncertainty of time-lapse image w/ joint method pJRM and 6 surveys. (f) Error of time-lapse image w/ pJRM and 6 surveys.

highlighted two key findings: first, joint recovery significantly enhances time-lapse signal reconstruction compared to its independently recovered counterpart; second, incorporating additional monitoring surveys further improves performance. Since this approach operates within a probabilistic framework it offers uncertainty analysis for the risk-averse application of CCS monitoring.

5 Acknowledgments

This research was carried out with the support of Georgia Research Alliance and partners of the ML4Seismic Center.

References

[1] Abhinav Prakash Gahlot, Mathias Louboutin, and Felix J. Herrmann. Time-lapse seismic monitoring of geological carbon storage with the nonlinear joint recovery model. In *International Meeting for Applied Geoscience and Energy*, 08 2023. (IMAGE, Houston).

[2] Reinhard Heckel and Paul Hand. Deep decoder: Concise image representations from untrained non-convolutional networks, 2019.

[3] Oscar Leong, Angela F Gao, He Sun, and Katherine L Bouman. Ill-posed image reconstruction without an image prior. *CoRR*, 2023.

[4] Olav Møyner, Grant Bruer, and Ziyi Yin. sintefmath/jutuldarcy.jl: v0.2.3, April 2023.

[5] Felix Oghenekohwo and Felix J. Herrmann. Compressive time-lapse seismic data processing using shared information. In *CSEG Annual Conference Proceedings*, 05 2015. (CSEG, Calgary).

[6] Rafael Orozco, Ali Siahkoohi, Mathias Louboutin, and Felix J. Herrmann. Aspire: Iterative amortized posterior inference for bayesian inverse problems, 2024.

[7] Matteo Ravasi and Ivan Vasconcelos. Pylops—a linear-operator python library for scalable algebra and optimization. *SoftwareX*, 11:100361, 2020.

[8] Philip Ringrose. *Storage of Carbon Dioxide in Saline Aquifers: Building confidence by forecasting and monitoring*. Society of Exploration Geophysicists, 2023.

[9] Ziyi Yin, Mathias Louboutin, and Felix J Herrmann. Compressive time-lapse seismic monitoring of carbon storage and sequestration with the joint recovery model. In *SEG International Exposition and Annual Meeting*, page D011S145R001. SEG, 2021.